

# DECAY OF A SCALAR $\sigma$ -MESON NEAR THE CRITICAL END-POINT IN THE PNJL MODEL

*A.V. Friesen, Yu.L. Kalinovsky and V.D. Toneev*  
Join Institute for Nuclear Research, Dubna

Properties of a scalar  $\sigma$ -meson are investigated in the two-flavor Nambu-Jona-Lasinio model with the Polyakov loop. Model analysis of the phase diagram of strong interacting matter is performed. The temperature dependence of the  $\sigma \rightarrow \pi\pi$  decay width is studied at the zero chemical potential and near the critical end-point. The calculated strong coupling constant  $g_{\sigma\pi\pi}$  and the decay width are compared with available experimental data and other model results. Nonthermal enhancement of the total decay width is noted for the  $\sigma$  meson near the critical end-point when the condition  $m_\sigma \geq 2m_\pi$  is broken.

PACS 13.25.Jx, 25.75.Nq

## Introduction

The models of Nambu–Jona-Lasinio type [1, 2, 3, 4] have a long history and are used to describe the dynamics and thermodynamics of light mesons. This type of models gives a simple and practical example of the basic mechanism of spontaneous breaking of chiral symmetry and key features of QCD at finite temperature and chemical potential [5, 6, 7, 8, 9]. The behavior of a QCD system is governed by the symmetry properties of the Lagrangian, namely, the global  $SU_L(N_f) \times SU_R(N_f)$  symmetry which is spontaneously broken to  $SU_V(N_f)$  and the exact  $SU_c(N_c)$  local color symmetry. On the other hand, in a non-Abelian pure gauge theory, the Polyakov loop serves as an order parameter of a transition from the low temperature confined phase ( $Z_{N_c}$  symmetric) to the high temperature deconfined phase characterized by the spontaneously broken  $Z_{N_c}$  symmetry (PNJL model). In the PNJL model, quarks are coupled simultaneously to the chiral condensate and to the Polyakov loop, and the model includes the features of both the chiral and  $Z_{N_c}$  symmetry breaking. The model reproduces rather successfully lattice data on QCD thermodynamics. The use of the PNJL model is therefore reasonable for investigating the in-medium properties of mesons and their decays [10, 11].

The aim of this work is the investigation of the meson properties and  $\sigma$  decay near the critical end-point (CEP). In this letter, we discuss the decay process  $\sigma \rightarrow \pi\pi$  at the finite temperature  $T$  and chemical potential  $\mu$  in the framework the Nambu-Jona-Lasinio model with the Polyakov-loop (PNJL) that is believed to describe well the chiral properties and simulates a deconfinement transition. Our motivation here is to elaborate these features in a large region of the temperature  $T$  and quark chemical potential  $\mu$ , where a non-thermal enhancement of pions due to the  $\sigma \rightarrow \pi\pi$  decay may take place.

# 1 The model and the phase diagram

We use the two-flavor PNJL model with the following Lagrangian [12, 13, 14]

$$\mathcal{L}_{PNJL} = \bar{q} (i\gamma_\mu D^\mu - \hat{m}_0) q + G \left[ (\bar{q}q)^2 + (\bar{q}i\gamma_5\tau q)^2 \right] - \mathcal{U}(\Phi[A], \bar{\Phi}[A]; T), \quad (1)$$

where the covariant gauge derivative  $D_\mu \equiv \partial_\mu - iA_\mu$  with  $A^\mu = \delta_0^\mu A^0$ ,  $A^0 = -iA_4$  (the Polyakov calibration). The strong coupling constant is absorbed in the definition of  $A_\mu$ . At the zero temperature the Polyakov loop field  $\Phi$  and the quark field are decoupled. Here, the quark field  $\bar{q} = (\bar{u}, \bar{d})$ , current masses  $\hat{m} = \text{diag}(m_u, m_d)$ , Pauli matrices  $\tau = \sigma/2$  act in the two color flavor space and  $G$  is the coupling constant.

The gauge sector of the Lagrangian density (1) is described by an effective potential  $\mathcal{U}(\Phi[A], \bar{\Phi}[A]; T) \equiv \mathcal{U}(\Phi, \bar{\Phi}; T)$

$$\frac{\mathcal{U}(\Phi, \bar{\Phi}; T)}{T^4} = -\frac{b_2(T)}{2}\bar{\Phi}\Phi - \frac{b_3}{6}(\Phi^3 + \bar{\Phi}^3) + \frac{b_4}{4}(\bar{\Phi}\Phi)^2, \quad (2)$$

where

$$b_2(T) = a_0 + a_1 \left(\frac{T_0}{T}\right) + a_2 \left(\frac{T_0}{T}\right)^2 + a_3 \left(\frac{T_0}{T}\right)^3. \quad (3)$$

The parameter set is obtained by fitting the lattice results in the pure  $SU(3)$  gauge theory at  $T_0 = 0.27$  GeV [13, 14] and is given in Table 1.

$a_0$	$a_1$	$a_2$	$a_3$	$b_3$	$b_4$
6.75	-1.95	2.625	-7.44	0.75	7.5

Table 1: The parameter set of the effective potential  $\mathcal{U}(\Phi, \bar{\Phi}; T)$ .

Before discussing the meson properties, one should introduce the gap equation for constituent quark mass should be introduced. For describing the system properties at the finite temperature and density the grand canonical potential in the Hartree approximation is considered [13, 14]

$$\begin{aligned} \Omega(\Phi, \bar{\Phi}, m, T, \mu) &= \mathcal{U}(\Phi, \bar{\Phi}; T) + N_f \frac{(m - m_0)^2}{4G} - 2N_c N_f \int_{\Lambda} \frac{d^3p}{(2\pi)^3} E_p \\ &\quad - 2N_f T \int \frac{d^3p}{(2\pi)^3} [\ln N_{\Phi}^+(E_p) + \ln N_{\Phi}^-(E_p)], \end{aligned} \quad (4)$$

where  $E_p$  is the quark energy,  $E_p = \sqrt{\mathbf{p}^2 + m^2}$ ,  $E_p^\pm = E_p \mp \mu$ , and

$$N_{\Phi}^+(E_p) = \left[ 1 + 3 \left( \Phi + \bar{\Phi} e^{-\beta E_p^+} \right) e^{-\beta E_p^+} + e^{-3\beta E_p^+} \right]^{-1}, \quad (5)$$

$$N_{\Phi}^-(E_p) = \left[ 1 + 3 \left( \bar{\Phi} + \Phi e^{-\beta E_p^-} \right) e^{-\beta E_p^-} + e^{-3\beta E_p^-} \right]^{-1}. \quad (6)$$

Integrals in Eq. (4) contain the three-momentum cutoff  $\Lambda$ .

From the grand canonical potential  $\Omega$  the equations of motion can be obtained

$$\frac{\partial \Omega}{\partial m} = 0, \quad \frac{\partial \Omega}{\partial \Phi} = 0, \quad \frac{\partial \Omega}{\partial \bar{\Phi}} = 0, \quad (7)$$

and the gap equation for the constituent quark mass can be written as follows:

$$m = m_0 - N_f G \langle \bar{q}q \rangle = m_0 + 8GN_c N_f \int_{\Lambda} \frac{d^3 p}{(2\pi)^3} \frac{m}{E_p} [1 - f_{\Phi}^+ - f_{\Phi}^-], \quad (8)$$

where  $f_{\Phi}^+, f_{\Phi}^-$  are the modified Fermi functions

$$\begin{aligned} f_{\Phi}^+ &= ((\Phi + 2\bar{\Phi}e^{-\beta E^+})e^{-\beta E^+} + e^{-3\beta E^+})N_{\Phi}^+, \\ f_{\Phi}^- &= ((\bar{\Phi} + 2\Phi e^{-\beta E^-})e^{-\beta E^-} + e^{-3\beta E^-})N_{\Phi}^-, \end{aligned} \quad (9)$$

with  $E^{\pm} = E \mp \mu$ . The regularization parameter  $\Lambda$ , the quark current mass  $m_0$ , the coupling strength  $G$  and physics quantities to fix these parameters are presented in Table 2.

$m_0$ [MeV]	$\Lambda$ [GeV]	$G$ [GeV] $^{-2}$	$F_{\pi}$ [GeV]	$m_{\pi}$ [GeV]
5.5	0.639	5.227	0.092	0.139

Table 2: The model parameters and quantities used for their tuning.

The  $\sigma$  and  $\pi$  meson masses are the solutions of the equation

$$1 - 2G \Pi_{ps/s}(k^2) = 0, \quad (10)$$

where  $k^2 = m_{\pi}^2$  and  $k^2 = m_{\sigma}^2$  in pseudo scalar and scalar sectors, and  $\Pi_{ps/s}$  are standard mesonic correlation functions [7]

$$i\Pi_{\pi}(k^2) = \int \frac{d^4 p}{(2\pi)^4} \text{Tr} [i\gamma_5 \tau^a S(p+k) i\gamma_5 \tau^b S(p)], \quad (11)$$

$$i\Pi_{\sigma}(k^2) = \int \frac{d^4 p}{(2\pi)^4} \text{Tr} [iS(p+k) iS(p)]. \quad (12)$$

Both pion-quark  $g_{\sigma\pi\pi}(T, \mu)$  and sigma-quark  $g_{\sigma\pi\pi}$  coupling strengths can be obtained from  $\Pi_{ps/s}$ :

$$g_{\pi/\sigma}^{-2}(T, \mu) = \frac{\partial \Pi_{\pi/\sigma}(k^2)}{\partial k^2} \Big|_{\substack{k^2=m_{\pi}^2 \\ k^2=m_{\sigma}^2}}. \quad (13)$$

As is seen from the gap equation (8), the quark condensate  $\langle \bar{q}q \rangle$  defines completely the quark mass in a hot and dense matter. This correlation is clearly demonstrated in Fig. 1, where the temperature dependence of the order parameters of the chiral condensate and the Polyakov loop, as well as the sigma

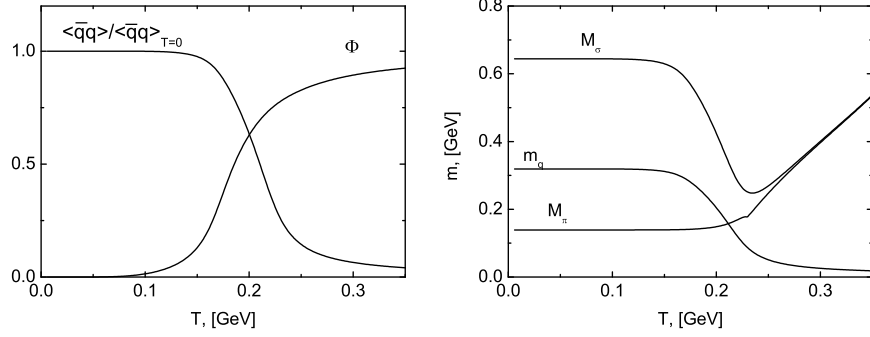


Figure 1: The temperature dependence of the chiral condensate and Polyakov loop (left panel) and particle masses (right panel) at  $\mu = 0$  within the PNJL model.

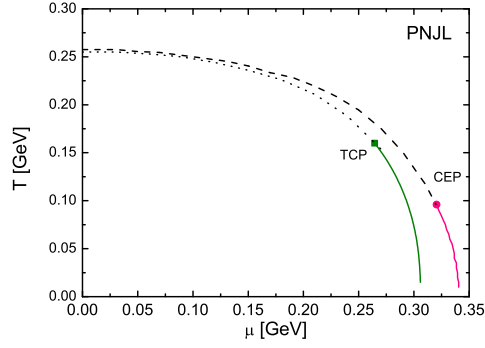


Figure 2: The phase diagram within the PNJL model. The solid lines denote the first-order transition boundary, the dotted line is the second-order transition and the dashed line is a crossover. The lines with the CEP and TCP points are calculated for a finite mass and in the chiral limit  $m_q = 0$ , respectively.

and pion masses are shown for  $\mu = 0$ . The pion hardly changes its mass and starts to become heavier only near  $T_c \sim 200$  MeV, while the sigma mass  $m_\sigma(T)$  decreases as the chiral symmetry gets restored, and eventually  $m_\pi(T)$  becomes larger than double quark mass  $m_q$  at the temperature  $T_{Mott} \sim 190$  MeV.

Since it is still difficult to extract certain information from the lattice simulations with the nonzero baryon density, we need QCD models for investigating the phase transitions at the finite baryon density. The calculated phase diagram of the physical states of matter within the PNJL model is given in Fig. 2. As is seen, in the real world with nonzero pion mass we have the first-order

phase transition at a moderate temperature and a large baryon chemical potential  $\mu_B = 3\mu$  that, with increasing  $T$ , terminates at the critical end-point  $(T_{CEP}, \mu_{CEP})$  where the second-order phase transition occurs. At a higher temperature  $T > T_{CTP}$  we have a smooth crossover. In the chiral limit with massless pions there is a tricritical point that separates the second-order phase transition at high temperature  $T$  and the first-order transition at lower  $T$  and high  $\mu$ . For the model parameters chosen (see Table 2) we obtain  $T_{CEP} \simeq 0.095$  GeV and  $\mu_{CEP} \simeq 0.32$  GeV (cf. with [15], where the critical temperature and chemical potential are calculated with the same parameters).

## 2 Decay $\sigma \rightarrow \pi\pi$

It is in order here to mention the significance of the scalar meson  $\sigma$  (a chiral partner of the pion) in QCD. A model-independent consequence of dynamic breaking of chiral symmetry is the existence of the pion and its chiral partner  $\sigma$ -meson: The former is the phase fluctuation of the order parameter  $\bar{q}q$  while the latter is the amplitude fluctuation of  $\bar{q}q$ . During the expansion of the system, the in-medium  $\sigma$  mass increases toward its vacuum value and eventually exceeds the  $2m_\pi$  threshold. As the  $\sigma \rightarrow \pi\pi$  coupling is large, the decay proceeds rapidly. Since this process occurs after freeze-out, the pions generated by it do not have a chance to thermalize. Thus, one may expect that the resulting pion spectrum should have a nonthermal enhancement at low transverse momentum.

To the lowest order in a  $1/N_c$  expansion, the diagram for the process  $\sigma \rightarrow \pi\pi$  is shown in Fig. 3. The amplitude of the triangle vertex  $\sigma \rightarrow \pi\pi$  can be obtained

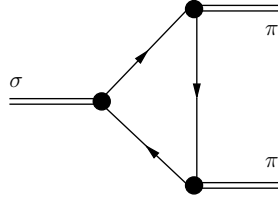


Figure 3: The Feynman diagram of the  $\sigma \rightarrow \pi\pi$  decay

analytically as

$$A_{\sigma\pi\pi} = \int \frac{d^4q}{(2\pi)^4} \text{Tr}\{S(q) \Gamma_\pi S(q+P) \Gamma_\pi S(q)\}, \quad (14)$$

where  $\Gamma_\pi = i\gamma_2\tau$  is the pion vertex function and  $S(q) = \hat{q} + m/\hat{q}^2 - m^2$  is the quark propagator, a trace is being taken over color, flavor and spinor indices.

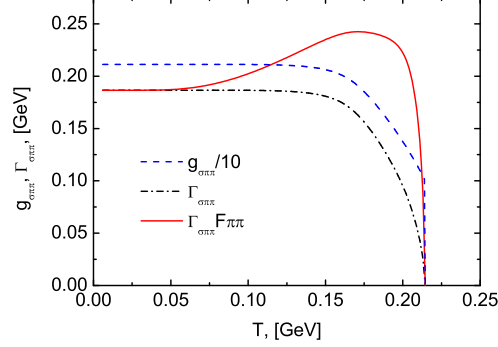


Figure 4: The temperature dependence of the total decay width  $\Gamma_{\sigma \rightarrow \pi\pi}$  and the coupling strength  $g_{\sigma\pi\pi}$  at the zero chemical potential. The solid and dash-dotted lines are the results for the decay width (16) with and without the Bose-Einstein factor  $F_{\pi\pi}$ , respectively.

After tracing and evaluation of the Matsubara sum one obtains [16, 17]

$$A_{\sigma\pi\pi} = 2mN_cN_f \int \frac{d^3q}{(2\pi)^3} \frac{(1 - f_{\Phi}^+ - f_{\Phi}^-)}{2E_q} \times \frac{(\mathbf{q} \cdot \mathbf{p})^2 - (2m_{\sigma}^2 + 4m_{\pi}^2)(\mathbf{q} \cdot \mathbf{p}) + m_{\sigma}^2/2 - 2m_{\sigma}^2E_q^2}{(m_{\sigma}^2 - 4E_q^2)((m_{\pi}^2 - 2(\mathbf{q} \cdot \mathbf{p}))^2 - m_{\sigma}^2E_q^2)}, \quad (15)$$

where  $f_{\Phi}^+$ ,  $f_{\Phi}^-$  are the modified Fermi functions (9). The coupling strength  $g_{\sigma\pi\pi}(T, \mu) = 2g_{\sigma}g_{\pi}^2A_{\sigma\pi\pi}(T, \mu)$ , where  $g_{\sigma}$  and  $g_{\pi}$  are coupling constants defined from Eq. (13)

The decay width is defined by the cut of the Feynman diagram in Fig.3 treating the sigma meson as a quark-antiquark system

$$\Gamma_{\sigma \rightarrow \pi\pi} = \frac{3}{2} \frac{g_{\sigma\pi\pi}^2}{16\pi m_{\sigma}} \sqrt{1 - \frac{4m_{\pi}^2}{m_{\sigma}^2}}. \quad (16)$$

The scalar meson  $\sigma$  can decay either into two neutral or two charged pions. All these channels are taken into account. The factor 3/2 in Eq.(16) takes into account the isospin conservation.

For the existing decay  $\sigma \rightarrow \pi\pi$  the kinematic factor  $\sqrt{1 - 4m_{\pi}^2/m_{\sigma}^2}$  in (16) leads to the constraint  $m_{\sigma} \leq 2m_{\pi}$  which is  $T$ - and  $\mu$ -dependent. One may expect that in the temperature region where this condition is broken the values  $g_{\sigma\pi\pi}$  and  $\Gamma_{\sigma \rightarrow \pi\pi}$  will drop to zero (Fig. 4). In the case  $\mu = 0$  considered the kinematic condition is broken at the  $\sigma \rightarrow \pi\pi$  dissociation temperature  $T_d^{\sigma} \approx 210$  MeV.

The coupling constant  $g_{\sigma\pi\pi}$  is about 2.1 GeV (note the scaling factor 1/10 in Fig.4) in vacuum and stays almost constant up to  $T \leq 0.22$  GeV (at  $\mu = 0$ )

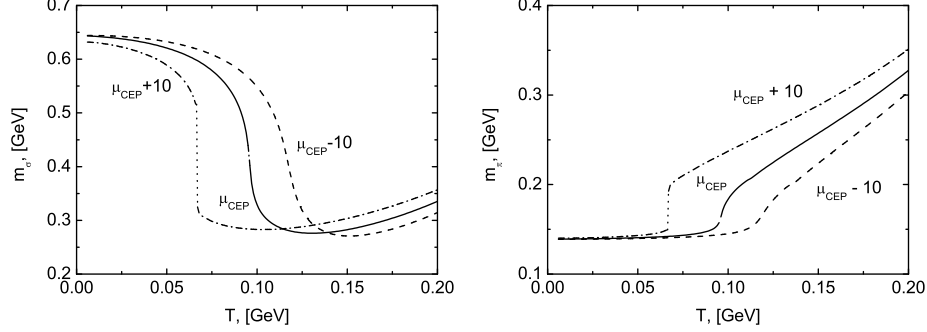


Figure 5: Temperature dependence of  $\sigma$  (left panel) and  $\pi$  (right panel) meson masses near the critical end-point. Solid lines correspond to the chemical potential at the critical end-point  $\mu_{CEP}$ . Dot-dashed and dashed lines are the PNJL results for  $\mu_{CEP} + 10$  and  $\mu_{CEP} - 10$  MeV, respectively. The dotted lines correspond to the mixed phase.

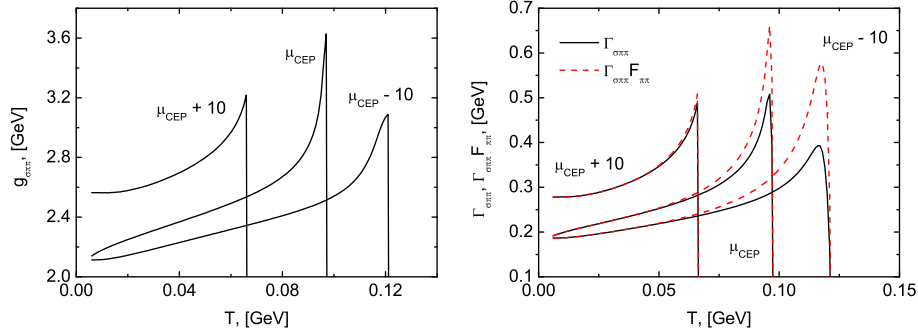


Figure 6: Left panel: The temperature dependence of the coupling strength  $g_{\sigma\pi\pi}$  at three values of the chemical potential  $\mu = \mu_{CEP}$ ,  $\mu_{CEP}-10$  MeV and  $\mu_{CEP}+10$  MeV. Right panel: The total decay width  $\Gamma_{\sigma \rightarrow \pi\pi}$  at the same values of chemical potentials. The total decay width  $\Gamma_{\sigma\pi\pi} F_{\pi\pi}$  and the width  $\Gamma_{\sigma\pi\pi}$ , Eq.(16) are plotted by the solid and dashed lines, respectively, for the same three values of  $\mu$ .

and then it drops to zero at  $m_\sigma = 2m_\pi$ . The experimental value, extracted from the  $J/\psi$  decays,  $g_{\sigma\pi\pi} = 2.0^{+0.3}_{-0.9}$  GeV [18] is in reasonable agreement with our result. It is of interest to note that the quark-meson models predict  $g_{\sigma\pi\pi} = 1.8$  GeV [19] and  $1.8^{+0.5}_{-0.3}$  GeV [20], and the linear sigma model gives  $g_{\sigma\pi\pi} = 2.54 \pm 0.01$  GeV [21].

The total  $\sigma$  decay width was measured recently in two experiments [18, 20,

22]. The Beijing Spectrometer (BES) Collaboration at the Beijing Electron-Positron Collider reported evidence of the existence of the  $\sigma$  particle in  $J/\psi$  decays. In the  $\pi^+\pi^-$  invariant mass spectrum in the process of the  $J/\psi \rightarrow \sigma\omega \rightarrow \pi^+\pi^-\omega$  they found a low mass enhancement, and the detailed analysis strongly favors  $O^{++}$  spin parity with a statistical significance for the existence of the  $\sigma$  particle. The BES measured values of the  $\sigma$  mass and total width are [18, 20]

$$m_\sigma = 390_{-36}^{+60} \text{ MeV}, \quad \Gamma_{\sigma \rightarrow \pi\pi} = 282_{-50}^{+77} \text{ MeV}. \quad (17)$$

The E791 Collaboration at Fermilab reported on evidence of a light and broad scalar resonance in the nonleptonic cascade decays of heavy mesons [19]. It was found in the Fermilab experiment that the  $\sigma$  meson is rather important in the  $D$  meson decay  $D \rightarrow 3\pi$  generated by the intermediate  $\sigma$ -resonance channel

$$m_\sigma = 478_{-23}^{+24} \pm 17 \text{ MeV}, \quad \Gamma_{\sigma \rightarrow \pi\pi} = 324_{-42}^{+40} \pm 21 \text{ MeV}. \quad (18)$$

These experimental values should be compared with  $\Gamma_{\sigma \rightarrow \pi\pi} \simeq 190$  MeV at  $T = \mu = 0$  (see Fig.4). One can additionally take into account the Bose-Einstein statistics of final pion states by introducing the factor  $F_{\pi\pi} = (1 + f_B(\frac{m_\sigma}{2}))^2$  [17] into the total decay width (16), where the boson distribution function  $f_B(x) = (e^{x/T} - 1)^{-1}$ . In contrast to the kinematic factor  $\sqrt{1 - 4m_\pi^2/m_\sigma^2}$ , this pion distribution function tends to increase the width. Near the Mott temperature  $\Gamma_{\sigma \rightarrow \pi\pi} \approx 250$  MeV at  $\mu = 0$ . In fact, the numerical calculation shows that  $\Gamma_{\sigma\pi\pi}(T)$  decreases as  $T$  goes up, and eventually vanishes at a high temperature. The measured widths (17),(18) are somewhat higher than that in our model at  $T = 0$ . It is noteworthy that the measured  $\sigma$  masses  $390_{-36}^{+60}$  [18] and  $478_{-23}^{+24}$  [22] are noticeably smaller than in our model  $m_\sigma \approx 620$  MeV (to be fixed by the model parameters) while the total decay width depends strongly on  $m_\sigma$ , see Eq.(16). The quark-meson models give the decay width that does not differ essentially from our estimate:  $\Gamma_{\sigma \rightarrow \pi\pi} = 173$  [19] and  $149.9$  [23] MeV though the used sigma meson mass is close to experimental ones, being  $m_\sigma = 485.5$  and  $478$  MeV, respectively.

The decay width was really not studied at the nonzero baryon density, in particular, in the region near the critical end-point. For the finite  $\mu$  the coupling strength and meson masses behave in a nontrivial way. Both  $\sigma$  and  $\pi$  mesons suffer a jump in the region of the first-order phase transition (see curve for  $\mu + 10$  MeV in Fig.5) which ends at the critical end-point  $\mu_{CEP}$  and then they change continuously for  $\mu < \mu_{CEP}$ , where the crossover-type phase transition occurs.

According to (16), this mass behavior defines the total decay rate of a  $\sigma$  meson at  $\mu \neq 0$ , as shown in the right panel of Fig. 6. As can be seen, the  $T$ -region of the decay enhancement becomes narrower with increasing  $\mu$ . The total widths  $\Gamma_{\sigma \rightarrow \pi\pi}$  and  $\Gamma_{\sigma \rightarrow \pi\pi} F_{\pi\pi}$  tend to grow with temperature exhibiting a narrow maximum due to particularities of the  $g_{\sigma\pi\pi}^2$  term in (16). The inclusion of the  $F_{\pi\pi}$  factor enhances this maximum, but this effect becomes smaller when one moves by  $\Delta\mu$  toward larger  $\mu$  from  $\mu_{CEP}$  because the pion mass increases above  $\mu_{CEP}$  (see Fig.5). If the chemical potential  $\mu = \mu_{CEP}$ , the temperature



at which coupling strength  $g_{\sigma\pi\pi}$  or total decay width  $\Gamma_{\sigma\rightarrow\pi\pi}$  drops down to zero, the temperature is just  $T = T_{CEP}$ . If  $\mu$  increases (decreases) with respect to  $\mu_{CEP}$  by  $\Delta\mu \sim 10$  MeV, the temperature decreases (increases), respectively, by about 30 MeV from  $T_{CEP}$ . Maximal values of  $\Gamma_{\sigma\rightarrow\pi\pi}$  near the critical end-point are larger than that for  $\mu = 0$  by a factor about 3. It means that a  $\sigma$  meson lives shorter in the dense baryon matter. The shape of  $g_{\sigma\pi\pi}(T)$  is insensitive to  $\mu$  around  $\mu_{CEP}$ . The full decay width  $\Gamma_{\sigma\rightarrow\pi\pi}$  exhibits some wide maximum near the temperature  $T_{CEP}$ . This maximum is enhanced due to the  $F_{\pi\pi}$  factor and gets more pronounced for smaller  $\mu$ .

## Concluding remarks

The two-flavor PNJL model that reasonably describes quark-meson thermodynamics at finite temperature and chemical potential is applied to calculate the  $\sigma \rightarrow \pi\pi$  decay in this medium. The emphasis here is made on the behavior near the critical end-point. At  $\mu = 0$  and  $T \rightarrow 0$  the coupling constant  $g_{\sigma\pi\pi} = 2.1$  GeV and the total  $\sigma$  decay width  $\Gamma_{\sigma\rightarrow\pi\pi} \approx 190$  MeV are in reasonable agreement with both available experimental data and quark-meson model estimates. At finite quark chemical potential near the critical end-point the  $\Gamma_{\sigma\rightarrow\pi\pi}$  width shows a sharp maximum coming from a particular behavior of the coupling strength  $g_{\sigma\pi\pi}$ . The sigma mesons live here a shorter time than in the baryonless matter. The rapid decrease of  $\Gamma_{\sigma\rightarrow\pi\pi}$  at a high temperature is due to the phase space factor (see Eq.(16)). The account for the Bose-Einstein statistics in the final state pions (the factor  $F_{\pi\pi}$ ) results in the appearance of some nonthermal maximum of the decay width near  $T$  and  $\mu$  at which the kinematic condition  $m_\sigma \leq 2m_\pi$  is broken. This width enhancement is about  $\sim 20\%$  at  $\mu_{CEP}$  and is negligible if one moves to  $\mu = \mu_{CEP} + \Delta\mu$ .

The presented results are obtained in the first order in the  $1/N_c$  expansion. In a more realistic case the  $\sigma - \omega$  and  $\sigma - A_1$  mixing can affect noticeably the considered quantities, especially for the  $\mu \neq 0$  case [24]. However, it corresponds to higher orders in  $1/N_c$ .

The measurements of nonthermal enhancement of pions might be considered as a signature of chiral phase transition. However, it is a difficult experimental problem since the  $\sigma$  life time is very short, and the pion contribution from the resonance decay should be separated carefully. So a more elaborated analysis is needed.

## Acknowledgments

We are grateful to P. Costa, E.A. Kuraev, V.V. Skokov, and M.K. Volkov for useful comments. V.T acknowledges the financial support within the ‘‘HIC for FAIR’’ center of the ‘‘LOEWE’’ program and Heisenberg-Landau grant. The work of Yu. K. was supported by the RFFI grant 09-01-00770a.

## References

- [1] *Ebert D., Volkov M. K.* Composite-meson model with vector dominance based on U(2) invariant four-quark interactions // Z. Phys. C. 1983. V. 16, No 3. P. 205-210.
- [2] *Volkov M. K.*, Meson Lagrangians in a superconductor quark model // Ann. Phys. 1984. V. 157, No 1. P. 282.
- [3] *Ebert D., Reinhardt H.*, Effective chiral hadron lagrangian with anomalies and skyrme terms from quark flavour dynamics // Nucl. Phys. B. 1986. V. 271, No 1. P. 188-226.
- [4] *Volkov M. K.*, Low-Energy Meson Physics in the Quark Model of Superconductivity type // Sov. J. Part. and Nuclei. 1986. V. 17. P. 186; *Ebert D., Reinhardt H., Volkov M. K.*, Effective Hadron Theory of QCD // Prog. Part. Nucl. Phys. 1994. V. 33. P. 1-120.
- [5] *Volkov M. K., Radzhabov A. E.*, The Nambu-Jona-Lasinio model and its development // Phys. Usp. 2006. V. 49. P. 551-561.
- [6] *Vogl V., Weise W.*, Effective hadron theory of QCD // Prog. Part. Nucl. Phys. 1991. V. 27, P. 195.
- [7] *Klevansky S. P.*, The Nambu-Jona-Lasinio model of quantum chromodynamics // Rev. Mod. Phys. 1992. V. 64. P. 649-708.
- [8] *Hatsuda T., Kunihiro N.*, QCD phenomenology based on a chiral effective Lagrangian // Phys. Rep. 1984. V. 247, P. 221-367.
- [9] *Ebert. D. et. al.*, Mesons and diquarks in a NJL model at finite temperature and chemical potential // Int. J. Mod. Phys. A. 1993. V. 8. P. 1295-1312.
- [10] *Costa P., Ruivo M. C., Kalinovsky Yu. L.*, Pseudoscalar neutral mesons in hot and dense matter // Phys. Lett. B. 2003. V.560. P. 171-177.
- [11] *Costa P. et al.*, Pseudoscalar mesons in hot, dense matter // Phys. Rev. C. 2004. V. 70. 025204.
- [12] *Pisarski R. D.*, Quark-gluon plasma as a condensate of Z(3) Wilson lines // Phys. Rev. D. 2000. V. 62. 111501.
- [13] *Hansen H. et al.*, Mesonic correlations at finite temperature and density in the Nambu-Jona-Lasinio model with a Polyakov loop // Phys. Rev.D. 2007. V. 75. P. 065004.
- [14] *Ratti C., Thaler M. A., Weise W.* Phases of QCD: Lattice thermodynamics and a field theoretical model // Phys. Rev. D. 2006. V. 73. P. 014019.
- [15] *Friesen A. V., Kalinovsky Yu. L., Toneev V. D.*, Thermodynamics in NJL-like models // arXiv:1102.1813.

- [16] *Hüfner J. et al.* Hadronisation cross-sections at the chiral phase transition of a quark plasma // Phys. Lett. B. 1994. V. 337. P. 30-36.
- [17] *Zhuang P., Yang Z.*, Sigma Decay at Finite Temperature and Density // Chin. Phys. Lett. 2001. V. 18. P. 344-346; arxiv:nucl-th/0008041.
- [18] *Wu N.*, BES R measurements and  $J/\psi$  decays // hep-ex/0104050.
- [19] *Faessler A., Gutsche T., Ivanov M. A., Lyubovitskij V. E., Wang P.*, Pion and sigma meson properties in a relativistic quark model // Phys. Rev. D. 2003. V. 68. P. 014011 [arxiv:hep-ph/0304031]
- [20] *Huo W, Zhang X, and Huang T*,  $\sigma$  meson in  $J/\psi$  decays // 2002 Phys. Rev. D 65 097505 [arXiv:hep-ph/0112025].
- [21] *Dib C., Rosenfeld R.*, Estimating sigma meson couplings from  $D \rightarrow 3\pi$  decays, // Phys. Rev. D. 2001. V. 63. P. 11750.
- [22] *E791 Collaboration, Aitala E. M. et al.*, Experimental evidence for light and broad scalar resonance in  $D \rightarrow \pi^- \pi^+ \pi^+$  decay // Phys. Rev. Lett. 2001 V. 86. P. 770-774.
- [23] *Menchaca Maciel C.M., Morones Ibarra J.R.*, Statistical analysis of the sigma meson considered as two-pion resonance // arXiv: 1003.3493
- [24] *Saito K., Tsushima K., Thomas A. W.*, Spectral change of sigma and omega mesons in a dense nuclear medium // arxiv:nucl-th/9811031.